13th International Symposium on Turbulence and Shear Flow Phenomena (TSFP13)
Montreal, Canada, June 25–28, 2024

MULTIRESOLUTION ANALYSIS OF CONVERGENCE AND DIVERGENCE OF INERTIAL PARTICLE VELOCITY IN TURBULENCE

Thibault Maurel–Oujia
Institut de Mathématiques de Marseille
Aix-Marseille Université, CNRS
Marseille, France
and
Research Institute for Value-Added Information Generation
Japan Agency for Marine-Earth Science and Technology, Yokohama, Japan
thibault.oujia@univ-amu.fr

Keigo Matsuda
Research Institute for Value-Added Information Generation
Japan Agency for Marine-Earth Science and Technology, Yokohama, Japan
k.matsuda@jamstec.go.jp

Kai Schneider
Institut de Mathématiques de Marseille
Aix-Marseille Université, CNRS
Marseille, France
kai.schneider@univ-amu.fr

ABSTRACT

We study the multiscale dynamics of inertial particle clustering using three-dimensional DNS data of isotropic turbulence with inertial particles considering different Stokes numbers. We apply a tessellation-based technique and thus assign a volume to each point particle. The temporal rate of change of the volumes yields the divergence of the particle velocity (Oujia *et al.*, 2020; Maurel-Oujia *et al.*, 2024). We perform a multiresolution analysis of the divergence on unstructured discrete particle positions (Matsuda *et al.*, 2022). Thus the multiscale clustering dynamics is assessed and the spatial scales where clustering formation and destruction are most active, is determined for the different Stokes numbers.

INTRODUCTION

Particle-laden flows are commonly encountered in a wide range of natural and industrial applications, from rain formation in clouds to combustion in aeronautic engines (Brownlee, 1985; Shaw, 2003). Understanding the dynamics of such particles in turbulent flows is of paramount importance for modeling and prediction of various phenomena. The objective of this study is to explore the dynamics of inertial particles within isotropic turbulence, employing tessellation-based techniques over finite timescales. Understanding the velocities of these particles is key to decoding their behavior, specifically their tendencies to converge or diverge within turbulent clouds. The complexity arises from the fact that particle velocities are known only at discrete spatial locations, i.e. at the particle position. This constraint renders traditional grid-based methods, such as the Fast Fourier Transform, unsuitable because the particles follow a Lagrangian framework and are not located on a fixed Cartesian grid. To address this challenge, we employ tessellation techniques, such as Voronoi and Delaunay tessellations.

Voronoi tessellations have been previously employed for the study of preferential particle concentration Monchaux *et al.* (2010*a*). More recently, Oujia *et al.* (2020) utilized the changes in the volume of Voronoi cells to investigate particle divergence. Maurel-Oujia *et al.* (2024) then proposed an improved version using modified Voronoi tesselation and extended the method for computing curl and helicity of the particle velocity and moreover the full particle velocity gradient tensor. While these approaches offer valuable insights into particle behavior at a global scale, they do not fully account for the multiscale nature of turbulence. It is essential to understand how divergence contributes at different scales, and this is where multiresolution analysis, see e.g. Mallat (1989) comes into play. By employing multiresolution techniques on tessellations, as developed in Matsuda *et al.* (2022), we can dissect how particle behavior varies at multiple scales, enabling a more nuanced and deeper understanding of their dynamics. Unlike traditional methods, which provide a global view of divergence and convergence of particles, a multiresolution approach allows us to examine their properties at different scales of motion. For this purpose, we employ coarsening and refinement operators to create a multilevel description of the particle flow field and its corresponding divergence.

We introduce the application of multiresolution analysis specifically to the study of divergence in particle-laden turbulent flows. This allows us to gain insight into the scales at which divergence/convergence is most prevalent and how these scales interact to influence the overall particle dynamics.

The remainder of the manuscript is organized as follows: We first summarize the DNS flow data used for our analyses. Subsequently, we describe the tesselation-based methods employed to determine the divergence of the particle velocity and construct the multiresolution technique based on the Delaunay

tessellation of particle positions. Results are presented for different Stokes numbers. Finally, we draw conclusions and offer some outlook for future work.

DIRECT NUMERICAL SIMULATION

The particle-laden flow data are obtained from DNS of homogeneous isotropic turbulence (HIT) using the incompressible form of the Navier–Stokes equations for the fluctuating components of velocity and pressure. Specifically, the equations are solved within a 2π-periodic cube using a fourth-order finite-difference scheme. Large-scale forcing is employed to establish a statistically stationary turbulent flow. For details on the numerical method we refer to Matsuda *et al.* (2017).

The simulations are done with $N_g^3 = 512^3$ grid points and for a Taylor-microscale Reynolds number $Re_\lambda = 204$. The Reynolds number is defined as $Re_\lambda \equiv u'\lambda/\nu$, where ν is the kinematic viscosity and λ represents the Taylor microscale.

Uniformly distributed discrete point particles are introduced into the fully developed turbulent flow. In total $N_p = 1.07 \times 10^9$ fluid and inertial particles are evolved in the simulations. The dynamics of these particles are governed by Maxey's model for inertial heavy point particles with Stokes drag (Maxey, 1987). The inertial dynamics is controlled by the Stokes number, $St = \tau_p/\tau_\eta$, where τ_p denotes the particle relaxation time and τ_η refers to the Kolmogorov time. The equations for the particle position $\boldsymbol{x}_{p\,j}$ and its velocity $\boldsymbol{v}_{p\,j}$ are given as follows:

$$d_t \boldsymbol{x}_{p\,j} = \boldsymbol{v}_{p\,j} \text{ and } \quad d_t \boldsymbol{v}_{p\,j} = -\frac{\boldsymbol{v}_{p\,j} - \boldsymbol{u}_{p\,j}}{\tau_p}, \tag{1}$$

where $\boldsymbol{u}_{p\,j}$ is the fluid velocity at the particle position $\boldsymbol{x}_{p\,j}$. The subscript p denotes quantities at a particle position, and the subscript j refers to the particle identification number.

We performed simulations for seven different Stokes numbers, $St = 0.05$, 0.1, 0.2, 0.5, 1, 2, and 5. Note that particles with different Stokes numbers were tracked in an identical turbulent flow.

METHODS

In the following we briefly describe the method for computing the divergence of the particle velocity using tesselation of the particle position and the multiresolution transform on the tesselation graph.

Tessellation-based divergence

In Maurel-Oujia *et al.* (2024) we proposed a method for computing the divergence of inertial particle velocities through the examination of volume changes in modified Voronoi cells. This approach relies on the conservation equation for particle number density n, expressed as $D_t n = \partial_t n + \boldsymbol{v}\cdot\nabla n = -n\nabla\cdot\boldsymbol{v}$, where D_t denotes the Lagrangian derivative. Moreover, the method exploits the fact that the local density within a modified Voronoi cell n_p is inversely proportional to its volume V_p. By computing the modified Voronoi volume at two subsequent time instants t^k and $t^{k+1} = t^k + \Delta t$ with a time step Δt, the change in volume can be assessed. Eventually, the divergence of the particle velocity$\mathscr{D}(\boldsymbol{v}_p)$ can be computed as follows (Maurel-Oujia *et al.*, 2024):

$$\mathscr{D}(\boldsymbol{v}_p) = -\frac{1}{n_p} D_t n_p = \frac{2}{\Delta t}\,\frac{V_p^{k+1} - V_p^k}{V_p^{k+1} + V_p^k} \tag{2}$$

A detailed validation of the method can be found in Maurel-Oujia *et al.* (2024).

Multiresolution analysis on graphs

In our study, we extend the tessellation-based method for computing particle velocity divergence, as originally developed by Matsuda *et al.* (2022), by incorporating a multiresolution analysis. This approach allows us to examine the particle flow dynamics across different scales of motion and thereby we can extract meaningful information on the particle distribution and its divergence.

We employ a multiresolution analysis based on Delaunay tessellation graphs, which serves as an representation of particle neighbor cells in physical space. The graphs are constructed across multiple levels $l = 0, \ldots, L-1$, where the level index l increases as the scale becomes larger.

For graph coarsening, we adopt the half-edge collapse operator as outlined by Kobbelt *et al.* (1998). This operator merges one vertex with an adjacent vertex, and the choice of vertices to merge is based on the minimum volume attribute of the tessellation cells associated with them. The algorithm for this coarsening process involves a series of steps that mark and merge vertices, updating the volume values in the process to ensure volume conservation. As such, the updated volume value for a vertex shifted to level $l+1$ is given by $V_i^{l+1} = V_{2i}^l + V_{2i+1}^l$.

In terms of the wavelet transform on these graphs, we consider a signal $s_i^0 = s^0(x_{p,i})$ on discrete particle positions. The wavelet transform is based on the conservation equation $V_i^{l+1}\bar{s}_i^{l+1} = V_{2i}^l \bar{s}_{2i}^l + V_{2i+1}^l \bar{s}_{2i+1}^l$, where $\bar{s}_i^l$ is the signal at the i-th vertex on the graph at level l. The projection operator is defined as

$$\bar{s}_i^{l+1} = \frac{1}{V_i^{l+1}}\left(V_{2i}^l \bar{s}_{2i}^l + V_{2i+1}^l \bar{s}_{2i+1}^l\right). \tag{3}$$

For the prediction operator, we assume that the predicted signals at the finer level are the same as the projected signals at the coarser level, i.e., equal to $\bar{s}_i^{l+1}$. Consequently, the detail coefficients can be obtained by the difference between the original and predicted signals

$$d_i^{l+1} = \frac{V_{2i}^l}{V_i^{l+1}}(\bar{s}_{2i+1}^l - \bar{s}_{2i}^l). \tag{4}$$

The wavelet energy spectrum can be defined as

$$\mathscr{E}_s(k_V) = \frac{N_l M_2[\sigma_i^l d_i^l]}{(2\pi)^D \Delta k_V}. \tag{5}$$

The volume based wave number is defined as

$$k_V = \frac{\pi}{d_V}, \tag{6}$$

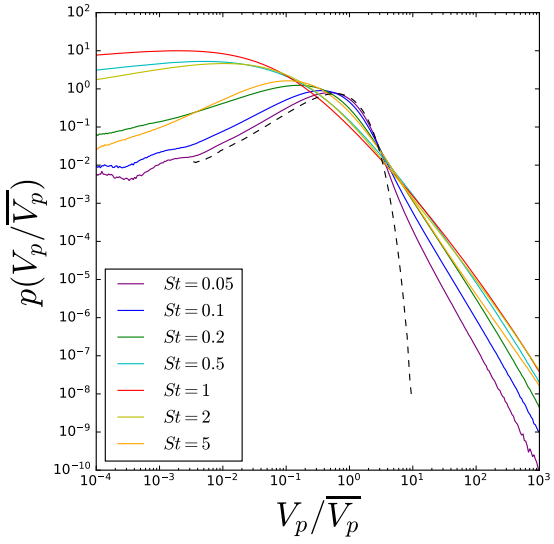

Figure 1: PDFs of volume of modified Voronoi tessellation normalized by the mean $V_p/\overline{V_p}$ for different Stokes numbers. The black dashed line represents the volume distribution in the case of randomly distributed particles.

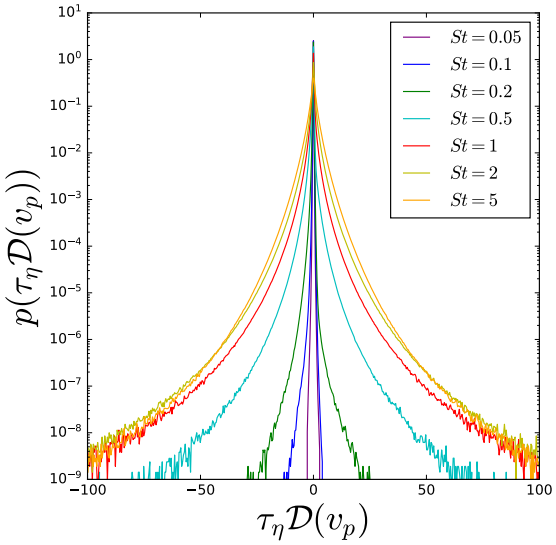

Figure 2: PDFs of the particle velocity divergence $\mathscr{D}(\boldsymbol{v}_p)$ for different Stokes numbers normalized by the Kolmogorov time scale τ_η.

where d_V is the mean volume scale, which is close to $2^{l/3}$. The bandwidth of the wavelets at each level l is Δk_V and $\sigma_i^{l+1} = \sqrt{V_i^{l+1} V_{2i+1}^l / V_{2i}^l}$ is the scaling factor required to achieve energy normalization, i.e in the L^2 norm. The term $M_2[d_i^l]$ is the second-order moment of the detail coefficients, computed as $M_2[d_i^l] = \frac{1}{N_l} \sum_{i=1}^{N_l} (d_i^l)^2$, where N_l is the total number of detail coefficients at level l.

RESULTS

First we explore the volume distribution of modified Voronoi tessellations. This allows to elucidate the effects of particle inertia on how particles are clustered. Figure 1 shows the PDFs of the volume of modified Voronoi tessellations normalized by the mean $V_p/\overline{V_p}$ for different Stokes numbers. Similarly to Monchaux *et al.* (2010*b*), we define cluster cells as cells that have a volume smaller than the left intersection value ($V_p/\overline{V_p} \approx 0.4$) of the PDF of the volume of inertial particles and the PDF of the volume of randomly distributed particles, and void cells as the cells that have a volume larger than the right intersection value ($V_p/\overline{V_p} \approx 3$). It can be observed that as the Stokes number increases and gets closer to 1, the number of small cells for $V_p/\overline{V_p} \lesssim 0.4$ increases, and then decreases after exceeding $St = 1$. This has also been observed in Dejoan & Monchaux (2013) and Baker *et al.* (2017) although here we show the volume of modified Voronoi cells and not that of the classical Voronoi. For larger cells, a similar behavior is observed, i.e., the number of large cells for $V_p/\overline{V_p} \gtrsim 3$ increases up to $St = 1$, and then slightly decreases. This illustrates the creation of void regions as the Stokes number increases, followed by their reduction as inertia continues to increase.

Figure 2 shows the PDFs of the particle velocity divergence $\mathscr{D}(\boldsymbol{v}_p)$ normalized by the Kolmogorov time scale τ_η for various Stokes numbers. The presented statistics are obtained by averaging over five different snapshots. The PDFs have a stretched exponential shape and the tails are getting heavier for increasing Stokes number. Table 1 quantifies the variance and flatness of the particle velocity divergence for different Stokes numbers. Variance offers insight into the average level of divergence fluctuation, while flatness, a fourth-order statistical moment, provides an indication of the distribution's tails. Specifically, high flatness values signify the presence of more statistically extreme events, characteristic of non-Gaussian and spatially intermittent behaviors. For a Gaussian distribution, the flatness value is equal to 3. For $St \leq 0.2$, variance and flatness of the particle velocity divergence show an increasing trend with the Stokes number. In turbulent flows, the divergence of particles for small Stokes numbers is predominantly driven by the fluid vorticity, mediated through centrifugal forces. When the Stokes number increases, it is expected that particles will exhibit a greater tendency to converge or diverge due to the large particle relaxation time which is consistent with our observations.

We note that for $St \geq 0.5$ the variance continues to increase, while the flatness begins to decrease. This observation can be attributed to the more random-like behavior of particles at higher Stokes numbers, where their inertial properties lead to more frequent crossing trajectories, i.e. the particle velocity becomes multi-valued, which is referred to as caustics (Wilkinson & Mehlig, 2005; Bec *et al.*, 2010). Consequently, particles, on the whole, are more likely to converge or diverge strongly. However, as this behavior is more generalized, these events are considered less statistically uncommon, resulting in a reduced flatness.

Figure 3 shows the wavelet energy spectrum of the particle velocity divergence for different Stokes number. The spectra are normalized by using the Kolmogorov scale η, the kinematic viscosity ν, and the energy dissipation rate ε. For $0.1 \leq St \leq 0.5$ the amplitude of the spectrum increases up to $k_V \eta \approx 0.5$, and then decreases along with the wave number. Additionally, an increase in the Stokes number leads to an increase in the spectrum amplitude. This phenomenon could be linked to the larger particle relaxation time, as already noted in the comments of figure 2. Moreover, the wave number with the maximum amplitude remains approximately the same for $0.1 \leq St \leq 0.5$, indicating no significant shift. This means that the scale of clustering or void formation does not change. In the cases $St \geq 1$, we see that for increasing Stokes number,

the overall amplitude of the spectrum also increases, and the wave number with the highest amplitude shifts to higher values, i.e., smaller scales. This may be attributed to caustics resulting from particle crossing phenomena which implies that the particle velocity becomes multi-valued. Moreover, particle crossings are pronounced at small scales. As the frequency of crossings increases with the Stokes number, the amplitude of the spectrum at high wave number likewise increases. The wavelet energy spectra thus show for $St = 5$ a power-law scaling similar to what is observed for random noise. We find the slope close to 1, which is similar to the slope observed for a Gaussian noise (Matsuda *et al.*, 2022).

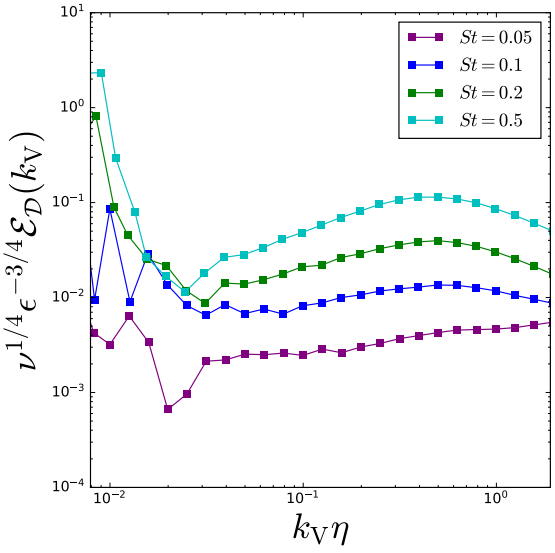

(a)

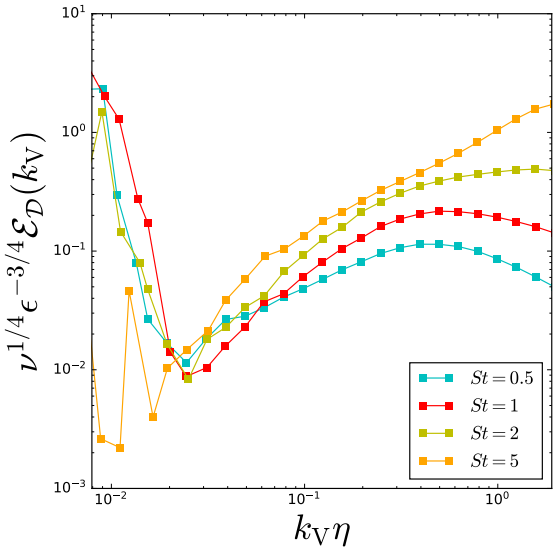

(b)

Figure 3: Wavelet energy spectrum of the particle velocity divergence $\mathcal{E}_{\mathcal{D}}(k_V)$ for small (a) and large (b) Stokes number.

CONCLUSIONS

We analyzed DNS data of particle laden isotropic turbulence for different Stokes numbers and assessed the multiscale clustering dynamics. To this end we applied tesselation based techniques which associate a volume to each point particle. Considering the temporal change of the volumes we determined the divergence of the particle velocity. Thus insights into cluster and void formation could be gained. Multiresolution representation of the particle tesselation yields then scale decomposition of the divergence. Therewith we can quantify the dynamics of cluster destruction and void formation at different scales of motion depending on the Stokes number. We found that the spectral distribution of energy does not change significantly. However the amplitude increases as the inertia increases which can be attributed to the τ_p dependence. Furthermore, the spectral distribution of energy does change, and an increase in amplitude for small scales is observed. We anticipate that this increase is due to more frequent particle crossing.

In future work we plan to compute not only the curl and the helicity of the particle velocity to quantify rotation and swirling motion in particle laden flows, but likewise the key tensor invariants, i.e. $\boldsymbol{Q}$ and $\boldsymbol{R}$, of the particle velocity gradient tensor. Compression and stretching of particle clusters can thus be quantified. Studying the influence of gravity onto particle settling and the related cluster formation is likewise object of future investigations.

Acknowledgments

T.M.O. and K.S. acknowledge funding from the Agence Nationale de la Recherche (ANR), grant ANR-20-CE46-0010-01. K.M. acknowledges financial support from JSPS KAKENHI Grant Number JP23K03686. K.S. acknowledges funding from the French Federation for Magnetic Fusion Studies (FR-FCM) and the Eurofusion consortium, funded by the Euratom Research and Training Programme under Grant Agreement No. 633053. The DNS data analyzed in this project were obtained using the Earth Simulator supercomputer system of JAMSTEC. T.M.O. acknowledges financial support from JSPS for a Short-term fellowship.

REFERENCES

Baker, Lucia, Frankel, Ari, Mani, Ali & Coletti, Filippo 2017 Coherent clusters of inertial particles in homogeneous turbulence. *Journal of Fluid Mechanics* **833**, 364–398.

Bec, J, Biferale, L, Cencini, M, Lanotte, AS & Toschi, F 2010 Intermittency in the velocity distribution of heavy particles in turbulence. *Journal of Fluid Mechanics* **646**, 527–536.

Brownlee, D.E. 1985 Cosmic dust: Collection and research. *Annu. Rev. Earth and Planetary Sciences* **13** (1), 147–173.

Dejoan, A. & Monchaux, R. 2013 Preferential concentration and settling of heavy particles in homogeneous turbulence. *Phys. Fluids* **25** (1), 013301.

Kobbelt, Leif, Campagna, Swen, Vorsatz, Jens & Seidel, Hans-Peter 1998 Interactive multi-resolution modeling on arbitrary meshes. In *Proceedings of the 25th annual conference on Computer graphics and interactive techniques*, pp. 105–114.

Mallat, Stephane G 1989 A theory for multiresolution signal decomposition: the wavelet representation. *IEEE transactions on pattern analysis and machine intelligence* **11** (7), 674–693.

Matsuda, Keigo, Onishi, Ryo & Takahashi, Keiko 2017 Influence of gravitational settling on turbulent droplet clustering and radar reflectivity factor. *Flow, Turbulence and Combustion* **98**, 327–340.

Matsuda, K., Schneider, K., Oujia, T., West, J., Jain, S. &

St	0.05	0.1	0.2	0.5	1	2	5
$\mathbb{V}(\tau_\eta \mathscr{D}(\boldsymbol{v}_p))$	0.0024	0.0042	0.0164	0.2307	1.1824	2.9149	5.9079
$\mathbb{F}(\tau_\eta \mathscr{D}(\boldsymbol{v}_p))$	16.172	70.370	328.64	314.30	155.97	54.608	18.646

Table 1: Variance $\mathbb{V}$ and flatness $\mathbb{F}$ of the particle velocity divergence $\mathscr{D}(\boldsymbol{v}_p)$ normalized by the Kolmogorov time scale τ_η for different Stokes numbers.

Maeda, K. 2022 Multiresolution analysis of inertial particle tessellations for clustering dynamics. In *Center for Turbulence Research, Proceedings of the Summer Program 2022*.

Maurel-Oujia, Thibault, Matsuda, Keigo & Schneider, Kai 2024 Computing differential operators of the particle velocity in moving particle clouds using tessellations. *Journal of Computational Physics* **498**, 112658.

Maxey, M. 1987 The gravitational settling of aerosol particles in homogeneous turbulence and random flow fields. *J. Fluid Mech.* **174**, 441–465.

Monchaux, R., Bourgoin, M. & Cartellier, A. 2010*a* Preferential concentration of heavy particles: a Voronoi analysis. *Phys. Fluids* **22** (10), 103304.

Monchaux, Romain, Bourgoin, Mickaël & Cartellier, Alain 2010*b* Preferential concentration of heavy particles: A Voronoï analysis. *Physics of Fluids* **22** (10).

Oujia, T., Matsuda, K. & Schneider, K. 2020 Divergence and convergence of inertial particles in high-Reynolds-number turbulence. *J. Fluid Mech.* **905**, A14.

Shaw, R. A. 2003 Particle-turbulence interactions in atmospheric clouds. *Annu. Rev. Fluid Mech.* **35** (1), 183–227.

Wilkinson, M & Mehlig, Bernhard 2005 Caustics in turbulent aerosols. *Europhysics Letters* **71** (2), 186.